LBL-35722
UC-414
Preprint

Lawrence Berkeley Laboratory

UNIVERSITY OF CALIFORNIA

Accelerator & Fusion Research Division

Submitted to Nuclear Instruments and Methods in Physics Research A

The Isochronous Storage Ring Free Electron Laser

K. LaMon

May 1994

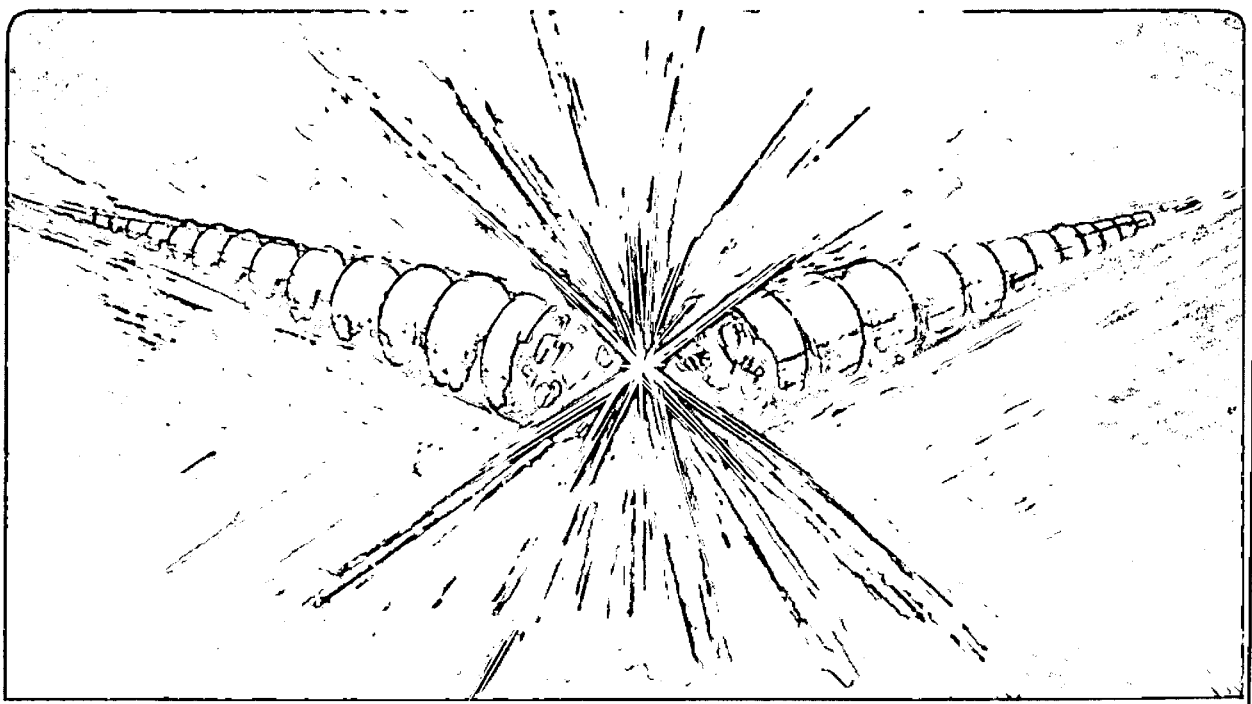

REFERENCE COPY
Does Not
Circulate
Bldg. 50 Library.
LBL-35722
Copy 1

Prepared for the U.S. Department of Energy under Contract Number DE-AC03-76SF00098

DISCLAIMER

This document was prepared as an account of work sponsored by the United States Government. While this document is believed to contain correct information, neither the United States Government nor any agency thereof, nor the Regents of the University of California, nor any of their employees, makes any warranty, express or implied, or assumes any legal responsibility for the accuracy, completeness, or usefulness of any information, apparatus, product, or process disclosed, or represents that its use would not infringe privately owned rights. Reference herein to any specific commercial product, process, or service by its trade name, trademark, manufacturer, or otherwise, does not necessarily constitute or imply its endorsement, recommendation, or favoring by the United States Government or any agency thereof, or the Regents of the University of California. The views and opinions of authors expressed herein do not necessarily state or reflect those of the United States Government or any agency thereof or the Regents of the University of California.

LBL-35722
UC-414

The Isochronous Storage Ring Free Electron Laser

Kenneth LaMon

Accelerator and Fusion Research Division
Lawrence Berkeley Laboratory
University of California
Berkeley, California 94720

May 1994

This work was supported by the Director, Office of Energy Research, Office of High Energy and Nuclear Physics, High Energy Physics Division, of the U.S. Department of Energy under Contract No. DE-AC03-76SF00098.

Abstract

The concept of an isochronous storage ring Free Electron Laser is studied using a simple model based on the longitudinal moments of the stored electron distribution. Laser performance is given as a function of machine parameters including momentum compaction and current density. Altogether, using the model presented we are able to calculate laser rise time, saturation characteristics, output power, and the time-dependent longitudinal profile of the optical laser pulses.

1. Introduction

At times the isochronous storage ring Free Electron Laser (FEL) has been looked upon as a possibility for creating a highly efficient storage ring FEL operating at near infrared wavelengths[1,2,3,4]. While the difficulty in constructing an isochronous storage ring has always been apparent, the potential rewards of such a SRFEL have continued to keep interest alive. After careful study and modeling, the results presented here taken from my recent Ph.D. thesis[5] demonstrate that based on laser performance taken together with parameter constraints the ISRFEL is not a worthwhile machine.

In the schematic design shown in Figure 1, electron bunches circulating inside the storage ring are timed to arrive synchronously (within a fraction of an optical wavelength) with the optical pulses contained in the laser cavity. As energy is transferred from the electrons to the light pulse the average energy spread $<\Delta\gamma/\gamma>$ of the electrons increases, eventually causing laser saturation. Because the ring is isochronous, electrons having different energies traverse the storage ring with virtually the same period. To appreciate the advantages of isochronicity we need to examine the FEL interaction which basically proceeds in two phases.

First the laser wave creates a longitudinal density modulation along the electron distribution, called microbunching, occurring on the scale of the optical wavelength. The modulated electron distribution then reacts resonantly with the optical field, amplifying it under proper circumstances. In a normal storage ring FEL the

microbunching is destroyed each pass by synchrotron oscillations as the electrons travel through the storage ring. However, in an isochronous storage ring the longitudinal profile of the electron distribution is preserved from pass to pass and hence the microbunching can be gradually enhanced after each traversal of the FEL. Clearly with prebunched electrons FEL gain could be increased by a few orders of magnitude. It might also be expected that with an isochronous ring one could reduce the rate of energy spread growth which leads to laser saturation in conventional storage ring FELs.

There are many difficulties associated with building an isochronous storage ring. Stability is more difficult to achieve than in an ordinary storage ring due to the reduced longitudinal focusing. Beam lifetime due to Touschek scattering[1,6,7] is also an important issue because of the reduced energy acceptance in an isochronous storage ring, placing an upper limit on the beam current in such a device.

Additionally, as one decreases the laser wavelength the tolerance requirements inside the storage ring become more and more stringent. Specifically, in order to achieve an isochronous SRFEL one must maintain a relative longitudinal slippage through the storage ring that is small compared with the laser wavelength. Hence the storage ring momentum compaction α must satisfy the relation:

$$\alpha \omega T \left\langle \frac{\Delta\gamma}{\gamma} \right\rangle < 1 \qquad (1.1)$$

where ω is the laser frequency, T is the period in seconds of the storage ring arcs, and $<\Delta\gamma/\gamma>$ is the average electron energy spread.

To describe the coupled electron bunch - optical field dynamics I present a one dimensional Vlasov model based around the pendulum equations of Colson[8]. The derivation below is taken from my thesis[5] where I also develop a separate, small signal model based on mapping equations for the lowest order moments of the electron distribution.

2. A Differential Equation Approach to FEL Simulation

The electron motion is described using longitudinal variables in phase $\zeta \equiv kz - \omega t$ and energy $\nu \equiv 4\pi N\, \Delta\gamma/\gamma$ where N is the number of undulator periods in the FEL. The electron energy γ is measured relative to the resonance energy γ_R defined by the well-known relation:

$$\lambda = \frac{\lambda_u}{2\gamma_R^2}(1 + K^2) \tag{2.1}$$

where λ is the laser wavelength λ_u is the undulator period and K is called the undulator parameter and is usually about unity.

The variables ζ and ν develop according to the single particle equations:

$$\dot{\zeta} = \nu \tag{2.2}$$

and $$\dot{\nu} = |a| \cos(\zeta + \phi) \tag{2.3}$$

The local amplitude $a \equiv |a| \exp(i\phi)$ of radiation field is described by:

$$\dot{a} = -j \left\langle e^{-i\zeta} \right\rangle \tag{2.4}$$

where j is the dimensionless electron current density. The brackets above indicate an average over the electron distribution on a length scale large compared with the optical wavelength yet much smaller than the electron bunch length. The pendulum equations (2.2) - (2.4) have a fairly wide range of validity, describing both strong and weak signal FEL operation[8,9].

To proceed, begin by writing down the Vlasov equation in one degree of freedom for the evolution of the electron distribution. The radiation field evolves according to the averaged Maxwell's equations (2.4). Essentially we are just converting the discrete particle approach of Colson into an equivalent continuous description using a distribution function. Thus we have:

$$\frac{\partial f(\zeta,\nu,\tau)}{\partial \tau} + \dot{\zeta} \frac{\partial f(\zeta,\nu,\tau)}{\partial \zeta} + \dot{\nu} \frac{\partial f(\zeta,\nu,\tau)}{\partial \nu} = 0 \tag{2.5}$$

where the dimensionless time variable τ has been defined so that a single traversal of the undulator corresponds to $\tau = 0 \rightarrow 1$.

Furthermore, we expand the distribution $f(\zeta,\nu,\tau)$ in terms of a

complete orthonormal basis in ζ and ν. The choice of the basis is determined by the assumed characteristics of the zeroth order electron distribution. Probably the most reasonable choice for $f(\zeta,\nu,\tau)$ is a finite Fourier series in phase ζ and an expansion in energy ν in terms of Chebyshev[10] polynomials. In general we may then write:

$$f(\zeta,\nu,\tau) = \frac{1}{\sqrt{2\pi}\sigma}\exp\left(-(\nu-\bar{\nu})^2/2\sigma^2\right)[1 + \eta\, e^{i\zeta} + \eta_2\, e^{2i\zeta} + \text{c.c.} + \ldots]$$

$$+\frac{1}{\sqrt{2\pi}\sigma^2} H_1\left(\frac{\nu-\bar{\nu}}{\sigma}\right)\exp\left(-(\nu-\bar{\nu})^2/2\sigma^2\right)[\, W\, e^{i\zeta} + W_2\, e^{2i\zeta} + \text{c.c.} + \ldots]$$

$$+\frac{1}{\sqrt{2\pi}\sigma^3} H_2\left(\frac{\nu-\bar{\nu}}{\sigma}\right)\exp\left(-(\nu-\bar{\nu})^2/2\sigma^2\right)[\, W_3\, e^{i\zeta} + W_4\, e^{2i\zeta} + \text{c.c.} + \ldots]$$

$$+\frac{1}{\sqrt{2\pi}\sigma^4} H_3\left(\frac{\nu-\bar{\nu}}{\sigma}\right)\exp\left(-(\nu-\bar{\nu})^2/2\sigma^2\right)[\, W_5 + \ldots] + \ldots \qquad (2.6)$$

where the orthogonal Chebyshev polynomials H are given by:

$$H_0 = 1\,, \quad H_1 = x\,, \quad H_2 = x^2 - 1\,, \quad H_3 = x^3 - 3x\,, \quad \ldots$$

In $f(\zeta,\nu,\tau)$ above the parameters $\bar{\nu}$, σ, η, W etc. are all assumed to be functions of time τ and slowly varying functions of ζ. The distribution $f(\zeta,\nu,\tau)$ above has the property that its phase space area is unity and also:

$$\langle\nu\rangle = \bar{\nu} \quad , \quad \langle(\nu - \bar{\nu})^2\rangle = \sigma^2 \quad \text{and} \quad \langle e^{-i\zeta}\rangle = \eta \qquad (2.7)$$

Notice that the coefficients of $H_1 e^{i0}$ and $H_2 e^{i0}$ in (2.6) are missing. The role of these two coefficients has been assumed by $\bar{\nu}$ and σ and they must be excluded to insure that $\bar{\nu}$ and σ do in fact represent the average energy and energy spread of the electron distribution.

Also from the definition (2.6) we have that:

$$W = \langle (\nu - \bar{\nu})\, e^{-i\zeta} \rangle \quad , \qquad W_3 = \langle ((\nu - \bar{\nu})^2 - \sigma^2) e^{-i\zeta} \rangle \tag{2.8}$$

The problem proceeds easier if we rewrite the Vlasov equation (2.5) in terms of the variable: $x \equiv (\nu - \bar{\nu})/\sigma$.

$$\frac{\partial f}{\partial \tau} + (x\,\sigma + \bar{\nu}) \frac{\partial f}{\partial \zeta} + \frac{1}{2\sigma} (a\, e^{i\zeta} + a^*\, e^{-i\zeta}) \frac{\partial f}{\partial x} = 0 \tag{2.9}$$

At this point we simply substitute the decomposition of $f(\zeta,\nu,\tau)$ in (2.6) into the Vlasov equation (2.5) and require that the coefficients of the resulting equation each vanish separately. For the moment terms we shall ignore terms proportional to $\partial/\partial\zeta$, which corresponds to taking the long bunch length limit. Setting the coefficient of $H_1 e^{i0}$ to zero in the resulting equation one obtains:

$$O(H_1 e^{i0}) : \qquad \dot{\bar{\nu}} = \frac{1}{2}(a^* \eta + a \eta^*) = \mathrm{Re}[\, a^* \eta \,] \tag{2.10}$$

Similarly at higher orders:

$$O(H_0 e^{i\zeta}) : \qquad \dot{\eta} = -i \bar{\nu} \eta - i W \tag{2.11}$$

$$O(H_2 e^{i0}) : \qquad \dot{\sigma}^2 = 2\,\mathrm{Re}[\,a^* W\,] \tag{2.12}$$

$$O(H_1 e^{i\zeta}) : \qquad \dot{W} = -i\,\bar{v}\,W + \frac{a}{2} - (\dot{\bar{v}} + i\,\sigma^2)\,\eta + \frac{1}{2}\eta_2\,a^* - 2\,i\,W_3 \tag{2.13}$$

From Equation (2.4) we have that the light pulse develops as:

$$\dot{a} = -j\,\eta \tag{2.14}$$

It is evident from these equations that the smallest set of variables needed to maintain a closed dynamical system while still having a physically interesting model includes: $\bar{v}$, σ^2, η, and W. We shall choose to neglect both η_2 and W_3 in equation (2.13) and in the rest of this discussion. Because η_2 represents bunching on half the usual scale any η_2 that gets built up during laser operation is damped away inside the storage ring at 4 times the rate at which η is damped (See derivation of Equation (3.8) below).

One must remember throughout this analysis that the electron bunch slips backward relative to the light pulse a distance $N\lambda$ in a single traversal of the undulator. If we assume that the length of the electron bunch and the light pulse are both long compared to the slippage distance $N\lambda$ then Equations (2.10) - (2.13) can be used to describe the evolution of the electron distribution at a particular phase.

The coupled problem in which long bunch length is not assumed, is best considered in two frames. The electron distribution

evolves in one frame while the light pulse is thought of to evolve separately in a different reference frame. To be more specific we should write for Equations (2.10) to (2.13):

$$\dot{\bar{v}}(\zeta,\tau) = \mathrm{Re}[\, a^*(\zeta-N\tau,\tau)\, \eta(\zeta,\tau)\,] \tag{2.15}$$

$$\dot{\eta}(\zeta,\tau) = -i\,\bar{v}\,\eta(\zeta,\tau) - i\,W(\zeta,\tau) \tag{2.16}$$

$$\dot{\sigma}^2(\zeta,\tau) = 2\,\mathrm{Re}[\, a^*(\zeta-N\tau,\tau)\, W(\zeta,\tau)\,] \tag{2.17}$$

$$\begin{aligned} \dot{W}(\zeta,\tau) = {} & -i\,\bar{v}(\zeta,\tau)\, W(\zeta,\tau) + \tfrac{1}{2} a(\zeta-N\tau,\tau) \\ & - (\dot{\bar{v}}(\zeta,\tau) + i\,\sigma^2(\zeta,\tau))\, \eta(\zeta,\tau) \end{aligned} \tag{2.18}$$

It is still reasonable at this level of approximation to ignore terms in $\partial/\partial\zeta$ while also including the affects of slippage in Equations (2.15) - (2.18). The neglected terms come into play at a slightly higher order than the retained longitudinal variations in the light pulse amplitude a.

For the time development of the radiation field we get instead of Equation (2.14):

$$\dot{a}(\zeta,\tau) = -\,j(\zeta+N\tau,\tau)\, \eta(\zeta+N\tau,\tau) \tag{2.19}$$

where $j(\zeta,\tau)$ is the local current density in the electron reference frame. Equations (2.15) - (2.19) can be integrated numerically to give the evolution of the coupled light pulse-electron bunch system

in the FEL. One integration scheme involves using one-dimensional arrays to represent the longitudinal profile of the electron bunch and light pulse. The light pulse array contains a as a function of position while the electron bunch array contains: $\bar{v}$, σ^2, η and W each as a function of longitudinal position within the bunch.

3. The Storage Ring Maps

To complete our description of isochronous storage ring FEL dynamics we must now derive equations equivalent to (2.10) - (2.13) for the development of the electron moments inside the storage ring. For brevity we will not discuss all the details of storage ring dynamics. For our purposes it is sufficient to characterize the storage ring as containing synchrotron radiation, momentum compaction and energy restoration. These three processes determine the period of synchrotron oscillation, the rate of synchrotron radiation damping, along with the electron bunch length and energy spread in equilibrium[7]. Because of low momentum compaction, the electron bunches in an isochronous storage ring have reduced bunch length and synchrotron frequency whereas equilibrium energy spread and the rate of storage ring damping remain unaffected. Because the rise time of the laser is assumed to be much shorter than the period of synchrotron oscillations we will ignore the affects of synchrotron oscillations from now on.

For the rest of this calculation we shall use the simplest of storage ring models, consisting first of a single cavity in which the

electrons receive a boost in energy $\Delta(n)$, with the amount of energy delivered varying according to the revolution number n. The energy replacement cavity is followed by simple arcs characterized by the nonlinear momentum compaction factor: $\alpha \equiv \alpha_1 + (\Delta\gamma/\gamma)\,\alpha_2$. In actuality the momentum compaction factor a can be expanded to arbitrary orders in energy and also emittance. For a complete discussion of this expansion and the relative importance of terms to the isochronous storage ring FEL see Deacon[1].

In terms of the longitudinal storage ring variables (ε,τ) the single particle storage ring maps may then be written:

$$\varepsilon' = \varepsilon + \Delta(n) \tag{3.1}$$

$$\tau' = \tau + \alpha_1 T\,\varepsilon' + \alpha_2 T\,\varepsilon'^2 \tag{3.2}$$

Here $\varepsilon = (\gamma - \gamma_s)/\gamma_s$ and τ represents relative time displacement along the electron bunch. Since we choose the storage ring design energy γ_s to coincide with the laser operating energy $\bar{\nu} = \pi$ we also have:

$$4\pi N \frac{\gamma_S - \gamma_R}{\gamma_R} = \pi$$

Converting Equations (3.1) and (3.2) into FEL variables gives:

$$\nu' = \nu + \Delta_\nu(n) \tag{3.3}$$

$$\zeta' = \zeta + \frac{\alpha_1 \omega T}{4\pi N}(\nu' - \pi) + \frac{\alpha_2 \omega T}{(4\pi N)^2}(\nu' - \pi)^2 \tag{3.4}$$

where T is the revolution period of the storage ring in seconds, N is the number of undulator periods, ω is the laser angular frequency.

Let us first derive the storage ring maps assuming perfect energy restoration before going on to the slightly more complicated case of imperfect energy restoration. For the case of perfect energy restoration $\Delta_\nu(n)$ in Equation (3.3) would be such that $\bar{\nu}' = \pi$ (operating energy) after every pass. In addition, Equation (3.4) becomes:

$$\zeta' = \zeta + \frac{\alpha_1 \omega T}{4\pi N} x\sigma + \frac{\alpha_2 \omega T}{(4\pi N)^2} x^2\sigma^2 \tag{3.5}$$

where we have defined: $x \equiv (\nu - \bar{\nu})/\sigma$.

To find the resulting storage ring map for the bunching parameter η, exponentiate Equation (3.5) above and integrate over the electron distribution $f(\zeta,\nu)$. We see from Equation (2.6) that the only non-vanishing terms after the integration over phase will be those proportional to η, W, W_3 etc.. That is:

$$\eta' = C_1 \eta + C_2 W + \ldots$$

where

$$C_1 = \int_{-\infty}^{\infty} \frac{dx}{\sqrt{2\pi}} e^{-x^2/2} \exp[-i\sigma x A - i\sigma^2 x^2 B] \tag{3.6}$$

and

$$C_2 = \frac{1}{\sigma}\int_{-\infty}^{\infty} \frac{dx}{\sqrt{2\pi}}\, x\, e^{-x^2/2} \exp[\,-i\,\sigma\, x\, A - i\,\sigma^2 x^2 B\,] \tag{3.7}$$

where we have used: $A \equiv \frac{\alpha_1 \omega T}{4\pi N}$ and $B \equiv \frac{\alpha_2 \omega T}{(4\pi N)^2}$.

Integrating and assuming also that $B\sigma^2 << 1$ we obtain for the bunching parameter map through the storage ring:

$$\eta' = (\eta - i\,A\,W)\exp(-A^2\sigma^2/2)\exp(-i\,\sigma^2 B) \tag{3.8}$$

To obtain the W map we use Equation (2.8). For perfect energy restoration we have that:

$$(\nu' - \bar{\nu}')e^{-i\zeta'} = ((\pi + \sigma\, x) - \pi\,)\, e^{-i\zeta'}$$

or

$$W' = \left\langle (\nu - \bar{\nu}) \exp(-i\zeta - i\,A\,x\,\sigma - i\,B\,x^2\sigma^2)\right\rangle_{\zeta,\nu}$$

Proceeding as before we notice that:

$$W' = i\frac{\partial}{\partial A}\eta' \quad .$$

This gives:

$$W' = \{\, W - i\,A\,\sigma^2(\eta - i\,A\,W)\,\}$$
$$\times \exp(-A^2\sigma^2/2)\exp(-i\,\sigma^2 B) \tag{3.9}$$

To proceed to the case of imperfect energy restoration we assume that the storage ring misses the operating energy $\bar{\nu} = \pi$ by an amount Δ. This gives for the first storage ring map:

$$\nu' = \pi + \Delta + x\sigma \tag{3.10}$$

The storage ring map for phase then becomes:

$$\zeta' = \zeta + A(\Delta + x\sigma) + B(\Delta + x\sigma)^2 \tag{3.11}$$

The integration is then quite straightforward, giving in the end:

$$\begin{aligned} \eta' = {} & (\eta - i(A + 2B\Delta)W)\exp(-(A + 2B\Delta)^2\sigma^2/2) \\ & \times \exp[-i(A\Delta + B(\Delta^2 + \sigma^2))] \end{aligned} \tag{3.12}$$

along with:

$$\begin{aligned} W' = {} & \{W - i\sigma^2(A + 2B\Delta)(\eta - i(A + 2B\Delta)W)\} \\ & \times \exp(-(A + 2B\Delta)^2\sigma^2/2)\exp[-i(A\Delta + B(\Delta^2 + \sigma^2))] \end{aligned} \tag{3.13}$$

4. Numerical Results

The SRFEL equations given above shall now be evaluated in the long bunch length limit ignoring slippage. The nominal values for machine parameters are: $\alpha_1 = 10^{-5}$, $\alpha_2 = 10^{-3}$, $N = 100$, $\lambda = 10^{-6}$ m

and $T = 10^{-7}$ s. The amplitude of the spontaneous radiation generated is calculated to be [11]: $|a_o| = 1.6 \times 10^{-4}$ while the phase of this radiation is made to vary randomly from pass to pass. Other parameter choices include the current density $j = 0.8$ along with the initial conditions: $\bar{v}(0) = 3.1416$, $\sigma^2(0) = 0.003$ and $\eta(0) = 0$.

Our first example is that of a lossless oscillator in which the undulator is enclosed by perfectly reflecting mirrors and a light pulse is built up inside the cavity over many passes starting from the spontaneous radiation. Note that in this first example no light is allowed to leave the laser cavity and that energy restoration in the storage ring is assumed to exactly compensate for the energy lost by the electrons to the light pulse. That is, the average electron energy $\bar{v}$ is set to the operating energy 3.1416 after every pass upon exiting the undulator. Additionally, the laser field amplitude a is given a phase change of π after each pass through the cavity by the electron bunch in order to restore the proper phase relation relative to the electron microbunching.

Figure 2a shows the logarithm of the magnitude of the radiation amplitude $|a|$ as a function of revolution number around the storage ring, while Figures 2b and 2c give the magnitude of the bunching parameter and the square of the energy spread in FEL units for this same example. The amplitude of the light pulse increases rapidly for the first 20 turns, after which point the energy spread has increased to where the storage ring begins rapidly to damp away the electron microbunching. The laser amplitude continues to increase with a reduced gain until growth stops after about 100 passes where $|a| \approx 3.7$, $\sigma^2 \approx 60$ and $\eta = 0$.

In contrast, Figure 3 displays the laser amplitude profile for the analogous conventional storage ring laser for which we have increased the momentum compaction α_1 so much that the ring is not at all isochronous and no microbunching is left over from pass to pass. Without isochronicity we see smaller gain, reaching maximum radiation amplitude after 250 turns, at which point: $|a| \approx 3.2$ and $\sigma^2 \approx 60$. Thus we reach basically the same final configuration as in the isochronous case, Figure 2a, but after about 150 additional turns. Figure 3 is not entirely accurate since in a conventional non-isochronous storage ring there would be bunch lengthening due to the increased energy spread.

5. Self-Amplified Single-Pass Operation

One of the most promising isochronous storage ring FEL configurations to consider and certainly the easiest to construct in practice occurs when we operate the FEL with no mirrors, external laser wave, and without energy restoration to the electrons. After every pass through the FEL the electrons create a new light pulse using the microbunching left over from the previous turn (See Equation (2.14)). As the microbunching η increases turn after turn so does the amplitude of the emitted light pulses. Operation is simplified since no thought has to be given to mirror alignment nor to keeping the phase of the microbunching commensurate with that of an external wave. In addition, energy restoration may be

neglected since the electrons are seen to lose only a small fraction of their energy.

Figure 4 shows the results of this mirrorless configuration with $j = 0.8$ and $\sigma^2(0) = 0.003$. Laser output is given as a function of revolution number for several values of the storage ring damping factor $A = \alpha_1 \omega T/4\pi N$ (See Equation (3.8)) with the nominal case defined as $A = 1.5$. Here simply by exploiting the isochronicity of the storage ring we see up to a 7 order of magnitude increase in the intensity of the emitted light pulses ($\approx |a|^2$) above the single-pass level produced in a conventional non-isochronous storage ring. Notice however that there is a limit placed on the maximum single-pass amplitude obtainable from the FEL. That is, because $|\eta| \leq 0.5$, by definition, we must then have from Equation (2.14) that $|a|_{max} \leq j/2$.

Although this configuration produces less total and peak power than in the mirrored case, here there is also only relatively mild energy spread growth in comparison. In Section 7 we are able to compare the merit of the two solutions more directly as we discuss SRFEL efficiency. What is surprising is that solutions with greater storage ring damping reach peak amplitude in less time and thereby have higher gain near startup. This phenomena appears to be due to coupling between the η and W moments in the storage ring.

6. Optical Pulse Narrowing

In Figures 5 and 6 we see the effects of the finite electron bunch length in this same mirrorless configuration. Elementary theory predicts that the electron bunches produced in a quasi-isochronous storage ring will be Gaussian and also shorter longitudinally than in conventional storage rings. Because the current density j is higher at the center of the electron bunch than at the ends, the laser interaction will consequently evolve faster at the center leading to an initial narrowing of the optical pulses (Figure 5). Later, as the energy spread at the center of the bunch causes local saturation, the outer unsaturated portions continue to provide gain giving the double humped optical pulse shown in Figure 6.

7. Equilibrium Solutions and SRFEL Efficiency

In his thesis Deacon[1] postulated that the isochronous storage ring FEL would operate in a continuous fashion of high gain even neglecting of the energy spread damping provided by synchrotron radiation in the storage ring. Using a simple one-dimensional model of the isochronous storage ring laser, Deacon derived conditions, based on machine parameters, for the existence of stable single particle fixed points, assuming a constant external radiation field (amplifier mode). Naturally the existence of fixed points does not ensure or predict laser gain. For this we require knowledge of the electron microbunching and its phase relation to the external radiation field.

The more detailed model presented here which takes into account energy spread growth and the formation of the electron microbunches shows that kind of equilibrium solution predicted by Deacon cannot exist in reality. With the inclusion of the longitudinal dimension into our model the situation becomes even more complicated. Due to slippage between the electrons and the light pulse, evolution at any given phase in the electron bunch is affected by the parameter values at adjacent locations. Also, the fact that the storage ring FEL interaction proceeds at different rates at different parts of the electron bunch illustrates further the impossibility of finding even a quasi-equilibrium solution for the entire bunch.

The more plausible type of equilibrium solution, often sought in conventional storage ring FEL models[12,13,14,15] recognizes that the laser interaction will increase the energy spread of the electron bunches. Equilibrium storage ring laser solutions then come about as a balance between energy spread growth caused by the laser and energy spread cooling provided by the storage ring arcs. For conventional storage ring FELs, the Renieri limit gives the relationship between laser power and the amount of radiation that must be given off as synchrotron radiation in the storage ring arcs in order to balance the energy spread growth generated by the laser.

Explicitly the Renieri limit says:

$$P_L = \chi \frac{1}{2N} P_{SYN} \tag{7.1}$$

where 1/2N is the homogeneous gain bandwidth and χ denotes efficiency, shown to be no more than unity for conventional storage ring free electrons lasers.

Because of the great disparity between synchrotron radiation power and laser power caused by the factor of 1/2N above, storage ring FELs generally operate as pulsed lasers. That is, the laser interaction is allowed to develop through many passes by the electrons until checked by laser saturation due to energy spread growth. The FEL must then be disconnected following saturation to allow the storage ring arcs to cool the electrons before resuming pulsed operation.

One of the central reasons for considering building an isochronous storage ring FEL was that by preserving the electron microbunching from pass to pass in the storage ring one could presumably overcome the Renieri limit, Equation (7.1) above. We may now calculate the efficiency χ for the different isochronous storage ring FEL operating configurations presented elsewhere[5].

To calculate the efficiency χ note that the storage ring damps electron energy spread according to the relation:

$$\sigma^2 = \sigma^2(0) \exp(-2U_o/E_s) \tag{7.2}$$

where U_o is the total amount of synchrotron radiation emitted in the storage ring arcs and E_s is the storage ring energy. Knowing the initial and final energy spread in the FEL operating profile one may then calculate the amount of synchrotron radiation U_o needed to restore the initial electron energy spread. Comparing U_o with the

amount of optical energy $\Delta\nu$ produced in the laser determines χ the storage ring FEL efficiency.

The amount of time needed for storage ring damping depends on how large an initial energy spread can be tolerated by the FEL without compromising laser performance. In the examples considered, an initial energy spread of $\sigma^2 = 0.02$ was found to still give good laser results. For the case of an FEL with lossless, non-transmitting mirrors and perfect energy restoration, similar to that presented in Figure 2, we obtain: $\Delta\nu = 8.2$, $\sigma^2(0) = 0.02$, $\sigma^2(SAT) = 58$. Thus giving an efficiency $\chi = 0.33$. This efficiency is the same for the non-isochronous case depicted in Figure 3 since both configurations end up emitting the same amount of energy at the expense of equal amounts of energy spread growth.

For simplicity we may rewrite the efficiency χ as:

$$\chi = \frac{\Delta\nu}{\pi} \ln\left(\frac{\sigma^2(SAT)}{\sigma^2(0)}\right)^{-1} \tag{7.3}$$

where again $\Delta\nu$ is the total, average electron energy lost in the FEL.

For the case of 50% transmitting mirrors we obtain, assuming perfect energy restoration: $\Delta\nu = 0.39$, $\sigma^2(0) = 0.02$, $\sigma^2(SAT) = 0.19 \rightarrow$ $\chi = 0.049$.

Lastly, for the mirrorless, single-pass configuration presented in Figure 4 using the nominal values for momentum compaction $A = 1.5$ we obtain: $\Delta\nu = 0.25$, $\sigma^2(0) = 0.02$, $\sigma^2(SAT) = 0.21 \rightarrow$ $\chi = 0.034$.

These efficiency results show that the isochronous storage ring FEL is in fact not a more efficient variety of storage ring FEL. In addition, altering machine parameters such as current density and isochronicity is not seen to improve machine efficiency an further. The isochronous device thus delivers the same laser energy after fewer revolutions by the electrons than in a conventional SRFEL, but not at a savings when it comes to energy spread growth.

8. Conclusion

Although the isochronous storage ring FEL has been shown to have an intriguing gain mechanism, the results given here and in my Ph.D. thesis indicate that its construction would not be worthwhile. Tolerance requirements in the storage ring eliminate the possibility of short laser wavelengths, which in turn implies that the storage ring be operated at low energy. Because of low electron energy, the ability of the storage ring to damp the laser induced electron energy spread is largely restricted. Additionally, because of low momentum compaction, the longitudinal storage phase space area is reduced thus greatly limiting the electron current. There also remain large problems still to be addressed concerning the difficulty of construction of an isochronous storage ring along with instability issues. Aside from this, the output laser power calculated here for the isochronous storage ring FEL should easily be exceeded by either conventional lasers or by a high powered linear accelerator operated together with a mirrored FEL cavity.

List of Figures:

Fig. 1: Schematic diagram of an isochronous storage ring FEL.

Fig. 2a: The amplitude of an optical pulse contained in a lossless cavity is plotted against revolution number assuming quasi-isochronous storage ring.

Fig. 2b: Corresponding bunching parameter growth accompanying Fig. 2a.

Fig. 2c: Mean-squared energy spread growth accompanying Fig. 2a

Fig. 3: Same configuration as Fig. 2a except that momentum compaction is taken to be large.

Fig. 4: Single-pass self-amplified FEL performance as a function of the storage ring damping parameter 'A'.

Fig. 5: Longitudinal optical field profiles for single-pass self-amplified operation.

Fig. 6 Longitudinal optical field profiles for single-pass self-amplified operation.

Figure 1: Schemematic design of an isochronous storage ring FEL

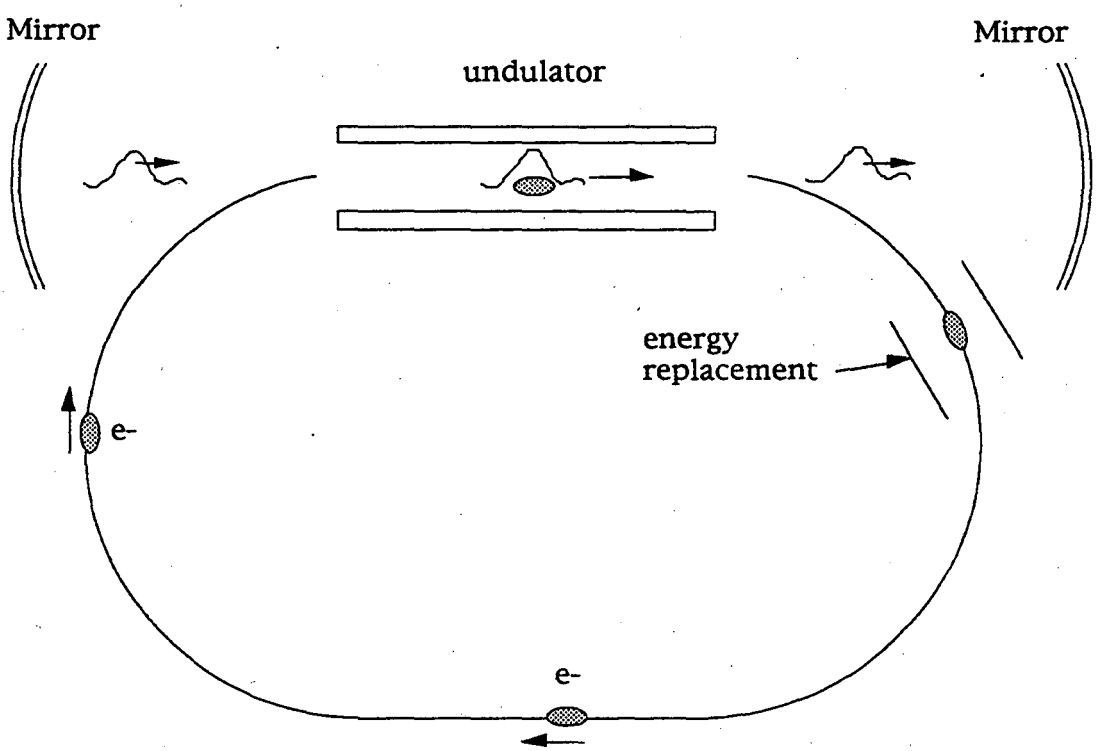

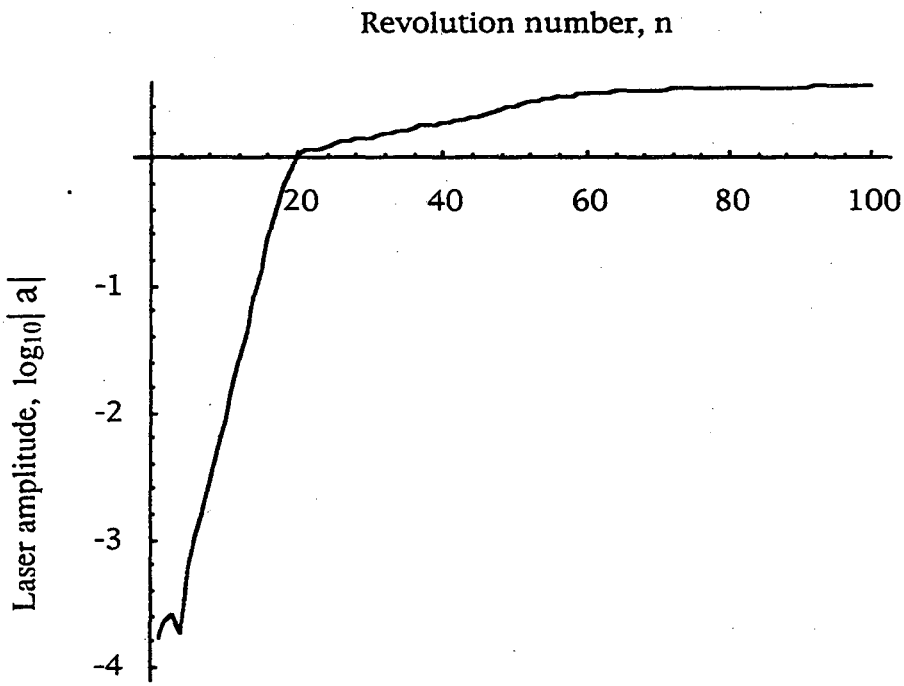

Figure 2a: Lossless oscillator configuration

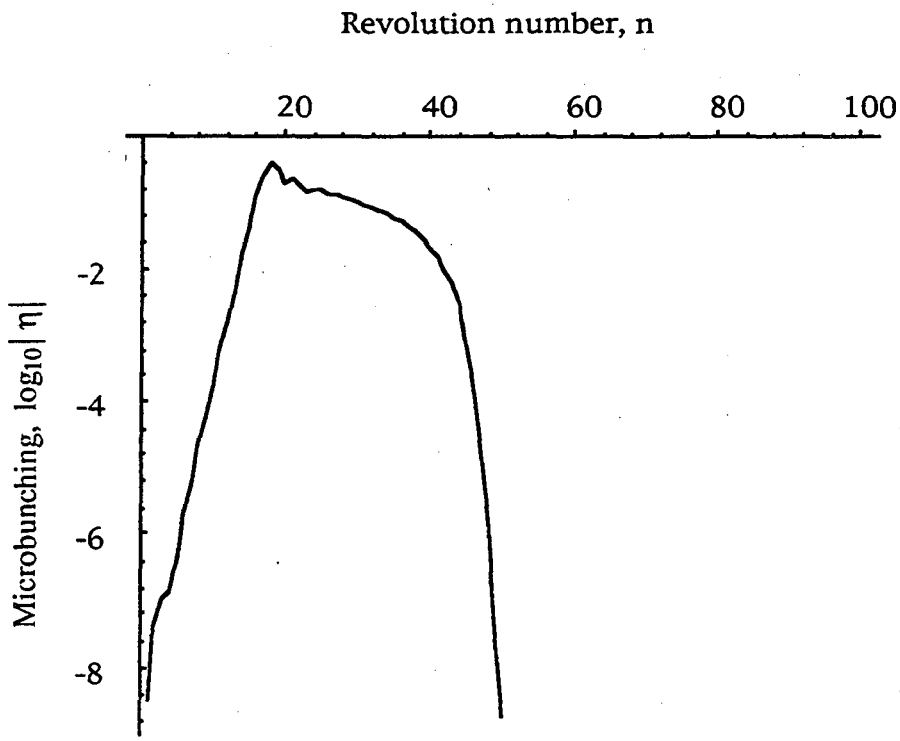

Figure 2b: Lossless oscillator configuration

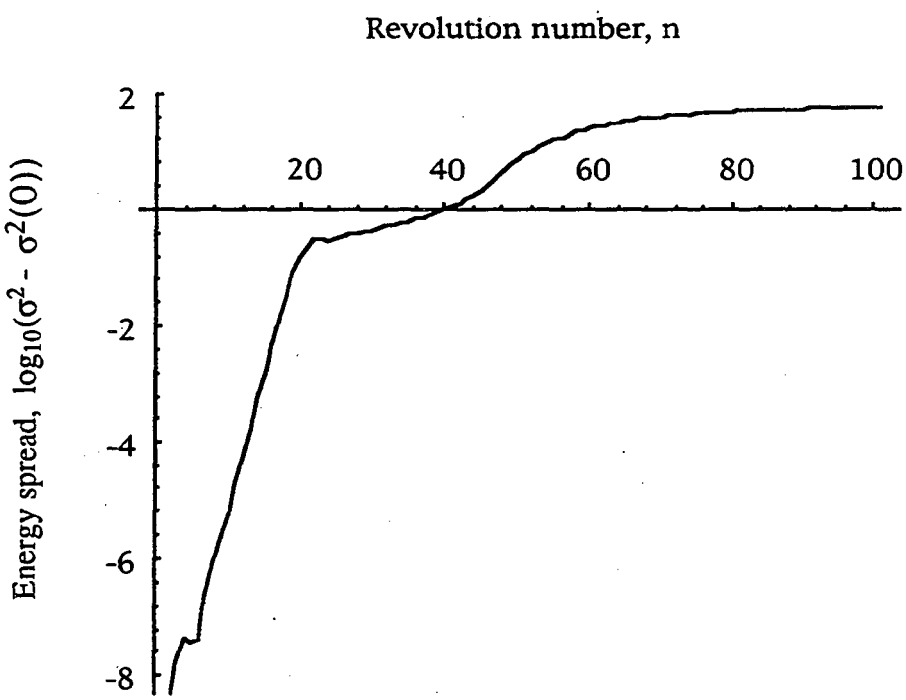

Figure 2c: Lossless oscillator configuration

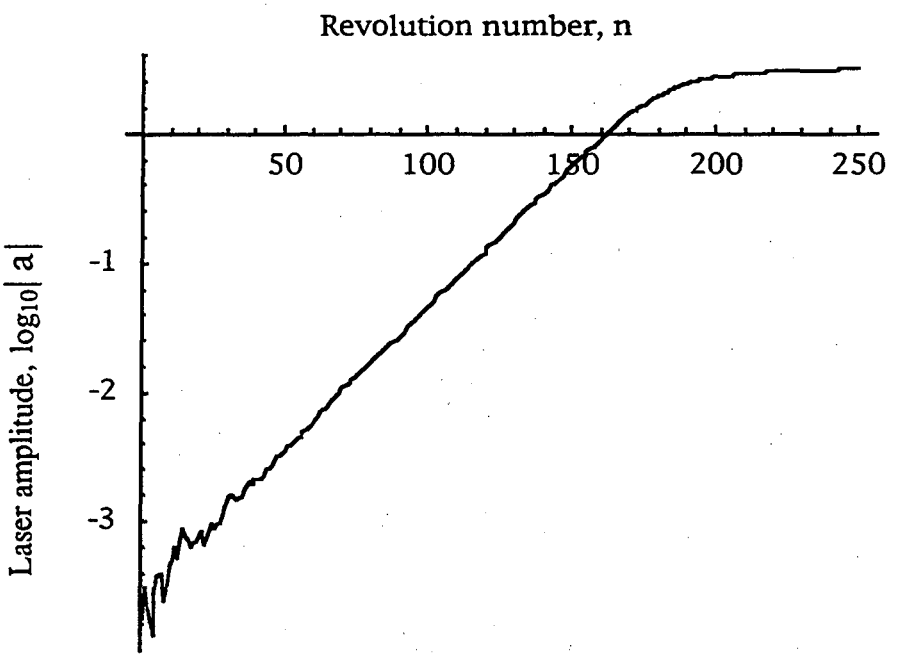

Figure 3: Conventional storage ring operation

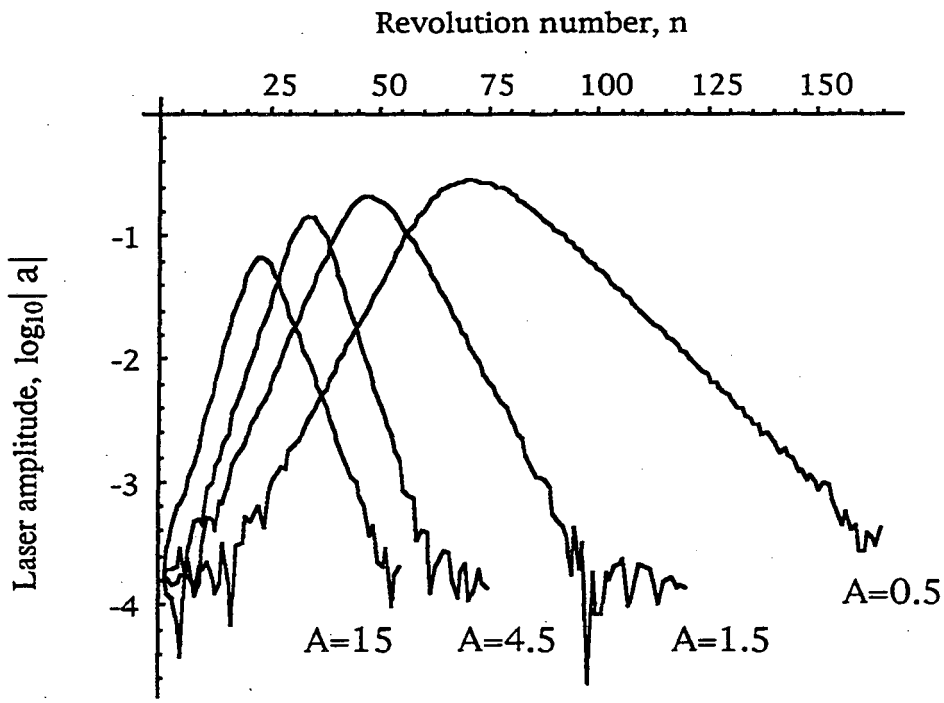

Figure 4: Self-amplified single-pass emission

Figure 5: Self-amplified single-pass emission, longitudinal light pulse profiles

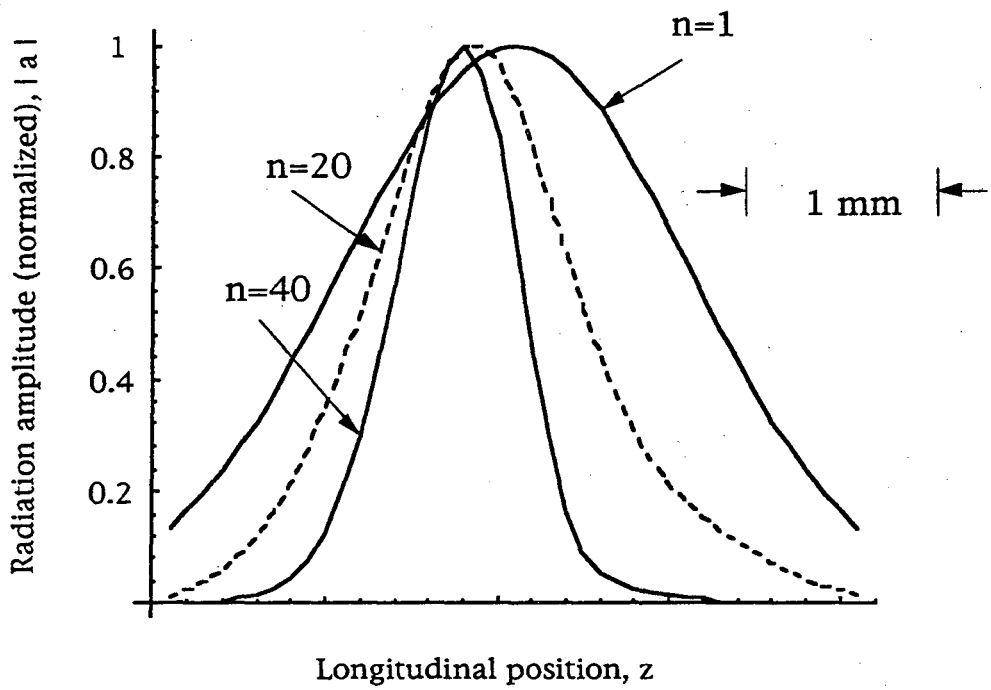

Figure 6: Self-amplified single-pass emission, longitudinal light pulse profiles

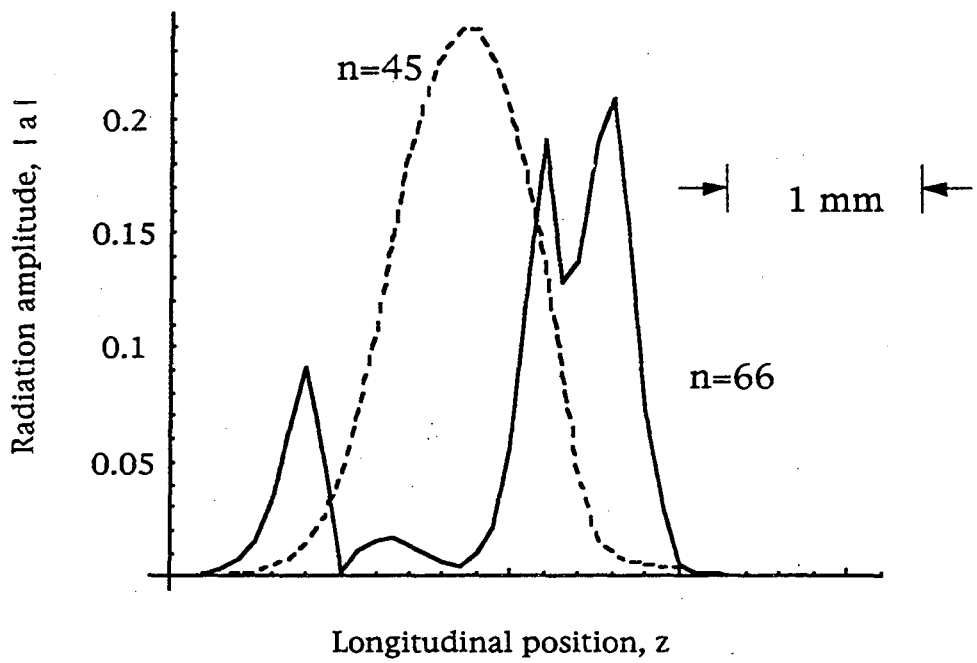

References:

1. D. Deacon, Ph.D. Thesis, Stanford, 1979.
2. D. Deacon, J. Madey, Phys. Rev. Lett. **44**, 449, 1980.
3. D. Deacon and J.M. Ortega, Ch. 10 in *Laser Handbook*, vol. 6, W. Colson et. al. editors, North-Holland, 1990, p. 361 - 362.
4. A. van Steenbergen, Ch. 12 in *Laser Handbook*, vol. 6, W. Colson et. al. editors, North-Holland, 1990, p. 446 - 449.
5. K. LaMon, Ph.D. Thesis, University of California, Berkeley, 1993.
6. H. Wiedemann, PEP Note 27, SLAC, Stanford, 1973.
7. M. Sands, in Proc. Intl. School of Physics, Course 46, ed. B. Touschek, Academic Press, N.Y., 1971, p. 256 - 411.
8. W. Colson, Ch. 3 in *Free Electron Laser Handbook*, W. Colson et. al. editors, North-Holland, 1990
9. C. Brau, *Free-Electron Lasers*, Academic Press, Inc., 1990.
10. I. Gradshteyn, I. Ryzhik, *Table of Integrals, Series, and Products*, Academic Press, Inc., New York, 1980.
11. K. J. Kim, **AIP 184**, 565, 1989.
12. A. Renieri, IEEE **NS-26**, 3827, 1979.
13. A. Renieri, Nuovo Cim. **53B**, 160, 1979.
14. G. Dattoli, A. Renieri, Nuovo Cim. **59B**, 1, 1980.
15. P. Elleaume, Journal de Physique **6**, 45, 1984.

LAWRENCE BERKELEY LABORATORY
UNIVERSITY OF CALIFORNIA
TECHNICAL INFORMATION DEPARTMENT
BERKELEY, CALIFORNIA 94720